Biotechnology Journal
www.biotechnology-journal.com

# Amorphous Polyphosphate and Ca-Carbonate Nanoparticles Improve the Self-Healing Properties of both Technical and Medical Cements

*Emad Tolba, Xiaohong Wang,* Shunfeng Wang, Meik Neufurth, Maximilian Ackermann, Heinz C. Schröder, and Werner E. G. Müller**

**Cement is used both as a construction material and for medical applications. Previously, it has been shown that the physiological polymer inorganic polyphosphate (polyP) is morphogenetically active in regeneration of skin, bone, and cartilage. The present study investigates the question if this polymer is also a suitable additive to improve the self-healing capacity not only of construction cement but also of inorganic bone void fillers. For the application in the cement, two different polyP-based amorphous nanoparticles (NP) are prepared, amorphous Ca-polyP NP and amorphous Ca-carbonate (ACC) NP. The particles are integrated into poly(methyl methacrylate) in a concentration ratio of 1:10. This material applied onto Portland cement blocks either by brush application or by blow spinning strongly accelerates the self-healing property of the cement after a 10 day incubation period. Most likely, this process depends on bacteria and their membrane-associated alkaline phosphatase, resulting in the formation of calcite from ACC. In a second approach, polyP is integrated into a calcium-silicate-based cement used in reconstitutive medicine. Subsequently, the cement becomes softer and more elastic. The data show that bioinspired polyP/ACC NP are suitable additives to improve the self-healing of construction cement and to biologize bone cement.**

## 1. Introduction

The progress of human civilization is accompanied by the development of innovations for the construction of temporary or permanent housings for demarcation and protection against the environment. Since the beginning of human history until today, over a period of several thousand years, durable buildings have been assembled or constructed, some of them still exist today. The oldest constructions date back to 12 000 BC in Israel[1] and are made of limestone and oil, components which are processed by spontaneous combustion to a natural and durable cement-like deposition. In parallel, the Babylonians and Assyrians likewise fabricated a natural binder by using bitumen together with bricks and gypsum for the plaster constructions.[2] The Egyptians improved this formulation by the addition of lime and gypsum mortar. Subsequently, the Greeks–Minoans used rough and curved limestone and selenite (gypsum) and filled the intermediate spaces with mortar of clay.[3] Later, the Romans developed a cement that allows the formation of sculptures and buildings that are remarkably durable, even if submersed underwater.[4] Examples from the ancient Greece period are shown in **Figure 1**. The Cretan palace of Knossos (2000 BC) was also built from bricks which show distinct leaching and weathering segments. In contrast to the high creep modulus for bending, the cement used during recent restoration

Dr. E. Tolba, Prof. X. H. Wang, Dr. S. Wang, Dr. M. Neufurth, Prof. H. C. Schröder, Prof. W. E. G. Müller
ERC Advanced Investigator Grant Research Group at the Institute for Physiological Chemistry
University Medical Center of the Johannes Gutenberg University
Duesbergweg 6, Mainz 55128, Germany
E-mail: wang013@uni-mainz.de; wmueller@uni-mainz.de

The ORCID identification number(s) for the author(s) of this article can be found under https://doi.org/10.1002/biot.202000101



Correction added on 16 July 2020, after first online publication: Projekt Deal funding statement has been added.

**DOI: 10.1002/biot.202000101**

Dr. E. Tolba
Polymers and Pigments Department
National Research Center
Dokki, Giza 12622, Egypt

Dr. M. Ackermann
Institute of Functional and Clinical Anatomy
University Medical Center of the Johannes Gutenberg University
Johann Joachim Becher Weg 13, Mainz 55099, Germany

Prof. H. C. Schröder
NanotecMARIN GmbH
Mühlstrasse 19, Ingelheim am Rhein 55218, Germany

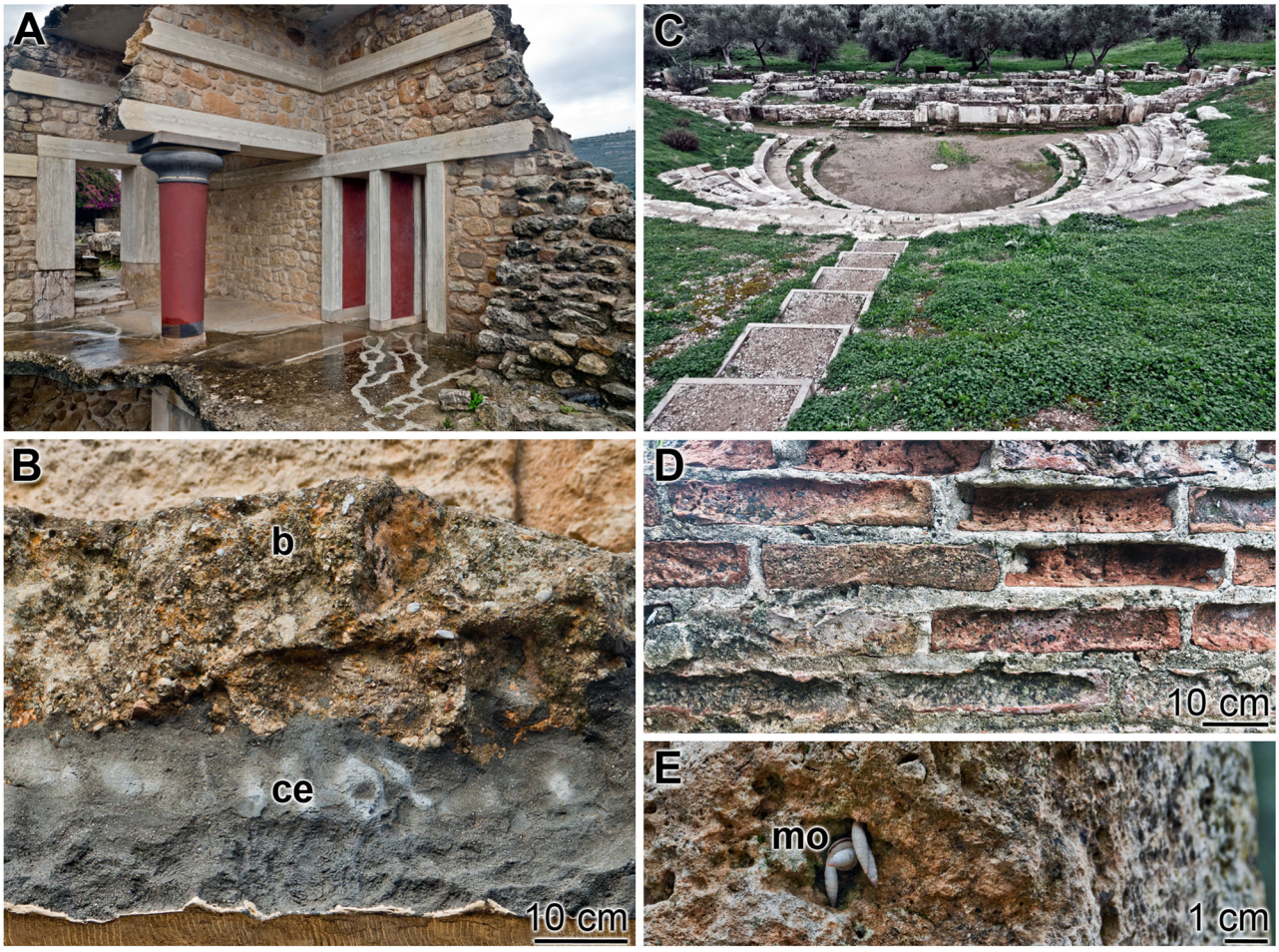


**Figure 1.** Brick and mortar samples at macroscale. A,B) Knossos. Cretan palace—Minoan period (2000 BC). A) Restored North Entrance with pillars (height: 2.20 m). B) The antique foundation bricks (b) which have been supported with present-day cement (ce) during the restoration. C–E) The ancient theater of Aptera (Greece, Crete) 8th century BC has been built of concrete faced with brick and then mortar. C) Theater: it has a total length of 55 m. D) Bricks with reinforcing joints made of recent cement. E) Grazing of mollusks (invertebrates) (mo) onto limestone-rich building blocks. The bricks (b), mortar (mo), and cement (ce) layers are marked.

periods is rigid and prone to crack formation (Figure 1A,B). From the 8th century BC is the ancient theater of Aptera (Greece, Crete). This large ancient theater has been built from bricks which contain high content of limestone (Figure 1C,D). This material is to a considerable portion composed of biogenic carbonate limestone that attracts invertebrates which feed/graze on the material and rasp down the carbonate with the radula of the animals to use this mineral for their exo-skeleton formation (Figure 1E).

The material used for construction of buildings by human civilization is a hybrid material, composed of a hard reinforcing component like sand or gravel (aggregate) and a binder, the cement, which is usually softer and hardens with time. If cement is mixed with fine aggregates, it forms the mortar for brickwork or if mixed with sand and gravel, it produces concrete.[5] Cement represents the most widely consumed inorganic material after water which ranks as number one on this planet. Often cements are inorganic ground substances that are based on lime, a calcium-containing mineral primarily composed of oxides and hydroxides, like calcium oxide and/or calcium hydroxide, or calcium silicate. The cements are the most essential component in the construction of buildings. It has been discovered already in the ancient times that burning of clay and stones is a suitable process to improve the quality of the cement for the fabrication of mortar. Among the most frequently applied cements is the Portland cement, discovered in 1824 by William Aspdin, which contains fine powder processed from limestone and clay by heating. An array of different modifications of cement has been developed, which is based on the use of additional admixtures like gypsum and the temperature for burning of the cement in the kiln.[6] Usually, a sintering temperature in the cement kiln of up to 1450 °C is applied to the raw mix. Under those conditions, the cement turns to a crystalline state which surely makes the material hard but also susceptible to impairments by microorganisms that are abundantly present in our environment. Just to remember approx. $10^5$ bacterial particles are present in 1 $m^{-3}$ of air, and those bacteria may cause corrosion of the concrete by their metabolic end products, like organic and inorganic acids that dissolve the integrity of the solid concrete components, followed by a deterioration of the material.[7]

A fully crystalline inorganic material, whether in dead or living systems, has no self-healing ability. In turn, both concrete used for the construction of houses (calcite, brownmillerite,

 

gypsum, calcite),[8] as well as mineralic inorganic deposits like bone (apatite)[9] are susceptible to bio-deterioration, unless living entities such as bacteria or cells are introduced in the crystalline minerals, cement, or bone, and change the crystalline phase to an amorphous one. In general, only the amorphous phase allows biogenic transformation and is prone to enzymatic changes which ultimately allow a re-organization (and repair) of cement or bone. Those self-healing processes proceed via enzymatic reactions and, in rare cases, exclusively via a thermodynamic downgrade.[10] This paradigm shift in the understanding of mineral deposition and self-repair has been introduced with silicatein, the first enzyme we discovered to be capable of catalyzing a mineral deposition, here of the skeletal elements of sponges, the spicules.[11] In a translational approach, we also succeeded in identifying two enzymes which are involved in bone mineral deposition, the carbonic anhydrase (CA) and the alkaline phosphatase (ALP) (reviewed in: ref. [12]). The latter enzyme is involved in the metabolism (degradation) of inorganic polyphosphate (polyP) which acts as a source of orthophosphate for bone mineral deposition and as a generator for metabolic energy in the form of ATP.[13,14]

PolyP is a natural polymer that is formed in every living cell.[15,16] A breakthrough toward the biomedical application was the discovery of how polyP can be fabricated as amorphous nanoparticles (NP) together with a corresponding divalent cation, like $Ca^{2+}$ or $Mg^{2+}$.[17] The functionally important aspect is that these polyP NPs have the same chemical composition and morphology like those found in eukaryotic cells, especially those in the polyP-storing intracellular compartments, the acidocalcisomes.[18] In turn, we outlined in a previous study that polyP is a new cornerstone for the improvement of cement formulation both for biomedical applications[10] and as a construction material.[19]

In addition to polyP as a major building block and energy supplier required for the stabilization of cement both for constructions and bone, $Ca^{2+}$-salts like Ca-carbonate are of great importance. It is well established that limestone, formed predominantly of calcite, is a crucial additive for Portland cements amounting to about 5 wt% of the cement.[20] This concentration is absolutely essential for keeping the stability of the cement.[21] It is established that cement used in ancient architecture is more durable and more resistant against a series of corrosive conditions, like freshwater, salt-water, seashore or salt-laden air, and hot spring water, while modern concrete composed of Portland cement suffers extensive damage under these conditions.[22] A major difference between ancient and modern cements is seen in the higher degree of carbonation in the ancient building material,[23] meaning the intensity and kinetics of the chemical reaction of carbon dioxide to produce carbonates, bicarbonates, and carbonic acid.

Based on this introduction, the key aspects to be considered for an improvement of cement for application both in medicine and building construction is the implementation first of polyP and second of Ca-carbonate into the starting material which have to be applied and fabricated as amorphous NP. A solution has been sketched already previously and applied for biological systems both in vitro and in vivo.[13,24] The basic concept of this technology was the successful stabilization ("freezing") of the amorphous phase of Ca-carbonate by inclusion of polyP during NP formation. In the present study, we prepared amorphous Ca-polyP/calcium carbonate NP ("Ca-polyP/ACC-NP") in a ratio of 20:80 (Ca-polyP:Ca-carbonate). These two components combine polyP, as a self-healing cement component,[19] with the precursor of the cement hardening calcite,[25,26] the amorphous calcium carbonate (ACC).

Closely related to cement for application as a construction material, cement for human medical use has been developed. While cement for the construction of buildings is based on lime or calcium oxide, silica, alumina, iron, and gypsum,[27] cement for application in human implants primarily contains calcium-silicate-based materials like the biodentine.[28] This formulation reacts in the presence of water and at high pH from tricalcium silicate ($3CaO{\bullet}SiO_2$; $C_3S$) to a hydrated calcium silicate gel ($3CaO{\bullet}2SiO_2{\bullet}3H_2O$; C-S-H) which surrounds the unreacted tricalcium silicate particles.[29] Importantly, biodentine reacts with water under the release of $Ca^{2+}$. The commercial biodentine formulation is delivered as a solid calcium-silicate-based cement which undergoes hardening in the presence of a Ca-chloride-containing liquid.[30] In the present study, this composition was used and exposed to polyP, either as soluble Na-polyP or as solid Ca-polyP nanoparticles. It has been postulated and subsequently confirmed that the $Ca^{2+}$ ions, released by biodentine, form strong mineralic deposits. This process has been attributed to a "fusing" of the calcium-silicate-based material with the polymeric polyP. Recently, it has been experimentally shown that the latter mechanism is correct.[31] It is the aim of the present study to elucidate if polyP, after encapsulation into particles, can be used for self-healing of construction cement and also for improvement of an augmentation material for medical implants.

## 2. Results

### 2.1. Characterization of the Nanoparticles

Two different formulations of nanoparticles (NP) were used in the present study: amorphous Ca-polyP-based NP and amorphous Ca-carbonate NP (ACC-NP). For the preparation of both formulations, a bioinspired translational approach was applied. The technology, previously introduced by us, was used.[17] During the preparation, the pH was kept constant at 10. Usually the ratio between solvent and solid material was 100:1.

#### *2.1.1. Ca-polyP-Based NP*

In all cells studied so far, polyP is deposited as ≈100 to 200 nm large amorphous particles.[32,33] All polyP chain lengths within those particles are medium-sized (≈40 phosphate units). We disclosed that those amorphous polyP particles can be synthesized if the divalent cation is applied to soluble polyP, like Na-polyP, in a super-stoichiometric ratio. The resulting particles, especially if $Ca^{2+}$ or $Sr^{2+}$ is used as cation, are amorphous and have a globular morphology. Within the particles, a myriad of channels from mesoporous components are arranged (reviewed in ref. [10]). A view into the characteristic preparation of NP using Na-polyP and $CaCl_2$ as starting compounds, "Ca-polyP-NP", with a size of around 50 nm (53 ± 11 nm) is given in **Figure 2**A.

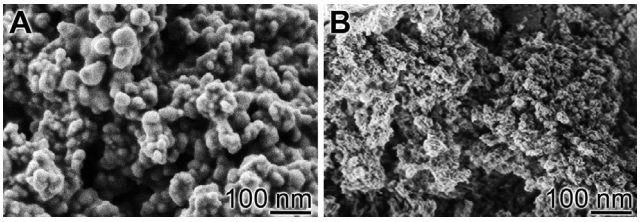


**Figure 2.** Morphology of the NP used in the present study. A) "Ca-polyP-NP," synthesized from Na-polyP and $CaCl_2$ as starting components; B) "ACC-NP" formed from $Na_2CO_3$ and $CaCl_2$; SEM.

#### 2.1.2. ACC-NP

In contrast to Ca-carbonate particles that are formed by precipitation from $CaCl_2 \bullet 2H_2O$ and $Na_2CO_3$ in the absence of polyP, which are crystalline (calcite, aragonite, or vaterite), the amorphous polymorph of Ca-carbonate is formed if polyP, as Na-polyP, at a concentration between 5% w/w and 10% w/w with respect to $Na_2CO_3$ and $CaCl_2$ is added to the starting compounds, "ACC-NP." The morphology of the particles is largely spherical with protrusions and a size of around 30 nm (17 ± 26 nm) (Figure 2B). For the studies reported here, polyP was added to Ca-carbonate in a concentration of 20% w/w. As documented before, the particles are largely amorphous by analyzing with X-ray diffraction (XRD).[13]

These particles were used for the improvement of the self-healing potency of the cement. Two methods for application were tested: brush application and blow spinning.

### 2.2. Inclusion of the Nanoparticles into Poly(methyl methacrylate): Brush Application

The unhydrated cement, "CEM", was mixed with water to obtain hydrated cement which was poured into circular 30 mm molds, as described under "Experimental Section." After a hardening period of 10 days (in a humid chamber) followed by an additional 1 day under room conditions, the specimens ("hCEM") were used for the experiments.

#### 2.2.1. Application onto Cement

The cement blocks were treated by brushing with either the polymer solution "PMMA" alone or with the solution of poly(methyl methacrylate) (PMMA) supplemented with 10 w/w% "Ca-polyP/ACC-NP" (based on PMMA). The latter formulation was termed "PMMA-Ca-polyP/ACC-NP." The respective polymer solution was applied with a paint roller, using ≈0.3 mL per 700 $mm^2$ of cement area. After drying for 60 min, the samples were inspected by environmental scanning electron microscope (ESEM) (**Figure 3**). The surface of the untreated cement sample "hCEM" showed the characteristic morphology of the hardened cement paste[34] with several crystalline structures (Figure 3A–C), including the flaky, flat-jagged calcium silicate hydrate (C-S-H) crystals and ettringite needles. In contrast, the surfaces of the cement samples coated with "PMMA" were smooth (Figure 3D,E) and showed only at the margins of the covering cement (Figure 3F). Supplementation of PMMA with the "Ca-polyP/ACC-NP" nanoparticles and a subsequent application of the obtained "PMMA-Ca-polyP/ACC-NP" solution onto the cement also provided a continuous layer which, however, showed the exposed nanoparticles (Figure 3G–I).

The depth of the penetration of the PMMA samples into the cement was assessed by electron microscopic (ESEM) inspection (**Figure 4**). The three different cement samples remained either untreated or were treated with the two PMMA formulations. In the absence of any treatment, no polymer was detected (Figure 4A,B). However, in the cement samples treated with "PMMA" (Figure 4C,D) or "PMMA-Ca-polyP/ACC-NP" (Figure 4E,F), an organic infiltration of ≈50 µm from the surface into the cement could be discerned.

#### 2.2.2. Dissolution of the PMMA Layer onto Cement

The durability of the PMMA layer onto the cement was determined before and after immersion of the samples into tap water for 2 days (**Figure 5**). The surface structure of the untreated "hCEM" samples with its crystal composition is shown in Figure 5A–C. After brush application of "PMMA-Ca-polyP/ACC-NP" to the cement samples, an almost continuous layer can be observed (Figure 5D–F). If those samples are submersed into water for 2 days (room temperature), large patches of ≈30 µm within the PMMA layer open and expose the cement substratum (Figure 5G–I).

#### 2.2.3. Self-Healing of Microcracks after "PMMA-Ca-polyP/ACC-NP" Application

Microcracks were introduced into "hCEM" after an aging period of 10 days by five consecutive freezing–thawing cycles. The microcracks introduced by this technique range within ≈15 and ≈58 µm in diameter. Those microcracks are characteristic initial damages, especially occurring in cultural heritage monuments,[35] the targets of our study.

After drying, those cement specimens remained either untreated or were treated with "PMMA" or "PMMA-Ca-polyP/ACC-NP" by brushing. After evaporation of the solvent the samples, cement blocks were submersed into water until its level reached 3 mm below the top edge of the blocks. The samples remained under those conditions for 10 days prior to microscopic inspection. Representative images are shown in **Figure 6**. They show that in the control assays, not treated with PMMA/polyP, the cracks do not show any process of self-healing (Figure 6A,B). The cracks are still bordered by sharp edges which frame the fissures. The cement samples which were covered with "PMMA" and then incubated for 10 days in a moist environment show first signs of self-healing after 10 days (Figure 6C,D). Within some areas of the cracks, newly formed material protrude into the crack space. This process is strongly accelerated if the cracks were overlayed with "PMMA-Ca-polyP/ACC-NP." In those samples, initially, almost the complete rays of cracks show or even complete closure of the cracks with newly deposited mineralic material (Figure 6E,F). At a higher magnification, it becomes apparent that the lately introduced globular particles are uniform and measure about 800 nm (Figure 6G,H).

 

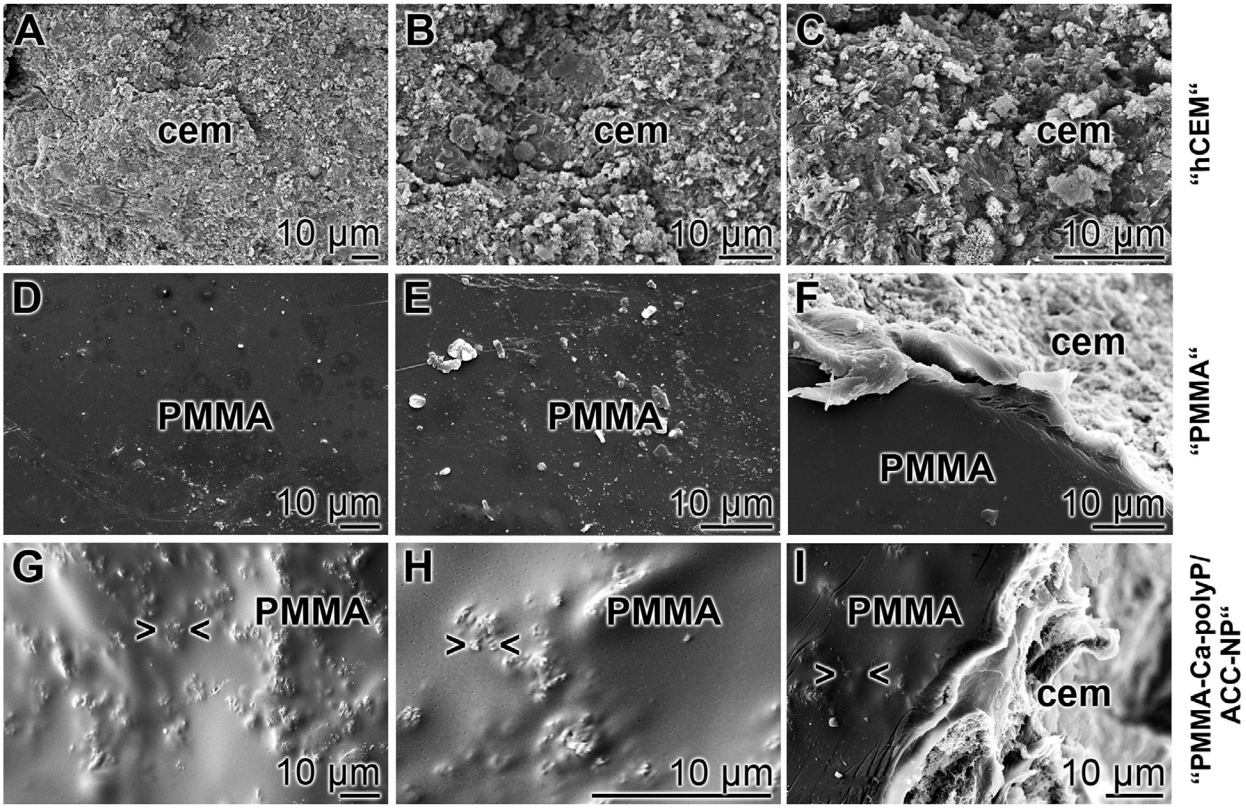


**Figure 3.** Surface morphology of the cement samples, "hCEM", which remained either A–C) uncovered or covered with D–F) "PMMA" or with G–I) "PMMA-Ca-polyP/ACC-NP"; ESEM. At the margins (F), the bare cement (cem) is occasionally seen below the polymer. The surfaces of the polymer (PMMA)-covered cement samples are smooth; if the polymer is supplemented with the polyP nanoparticles (> <), these particles are seen to protrude from the smooth surfaces.

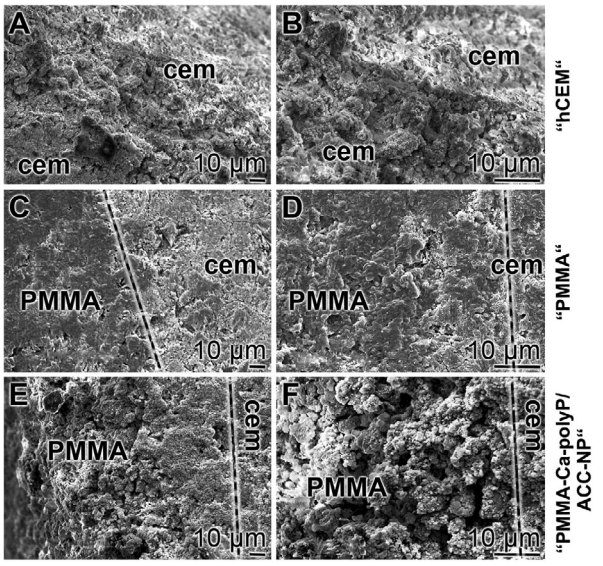


**Figure 4.** Assessment of the penetration depth of PMMA into the cement samples. Cement specimens were broken and the breaking edges were inspected by ESEM. In the untreated cement samples (A,B), no polymer infiltration could be seen. In contrast, if C,D) "PMMA" or E,F) "PMMA-Ca-polyP/ACC-NP" samples were studied, a penetration of the polymer into the cement by ≈50 µm could be discerned. A separation line (broken line) between the PMMA (PMMA) layer and the cement (cem) is given.

Preliminary determinations by energy-dispersive X-ray spectroscopy revealed a Ca, C, and P rich solid mineral-like deposition (preliminary results). Those particles are reminiscent of the nanoparticles added to the PMMA. In addition to the nanoparticle-like deposits, crystal structures are also seen (**Figure 7**) that appear to be ettringite[36] or calcite.[37]

### *2.2.4. Effect of the PMMA-Based polyP Coating on the Mechanical Properties of the Cement*

The hydrated cement samples, after hardening, were used for coating with PMMA, supplemented with polyP. The cement blocks were brushed only with the solvent, chloroform, or with "PMMA" or "PMMA-Ca-polyP/ACC-NP" as described under "Experimental Section." After evaporation of the solvent, the samples were subjected to nanoindentation using a Berkovich diamond indenter to determine their mechanical surface properties. The respective load-displacement curves are given in **Figure 8**A.

The curve load versus indentation depth (in nm) for the control cement sample, "hCEM", and the two coated sample series "PMMA" and "PMMA-Ca-polyP/ACC-NP" were calculated with respect to the Martens hardness (HM) and the Young's modulus (Er) using the Nano-Test Platform software package. The

 

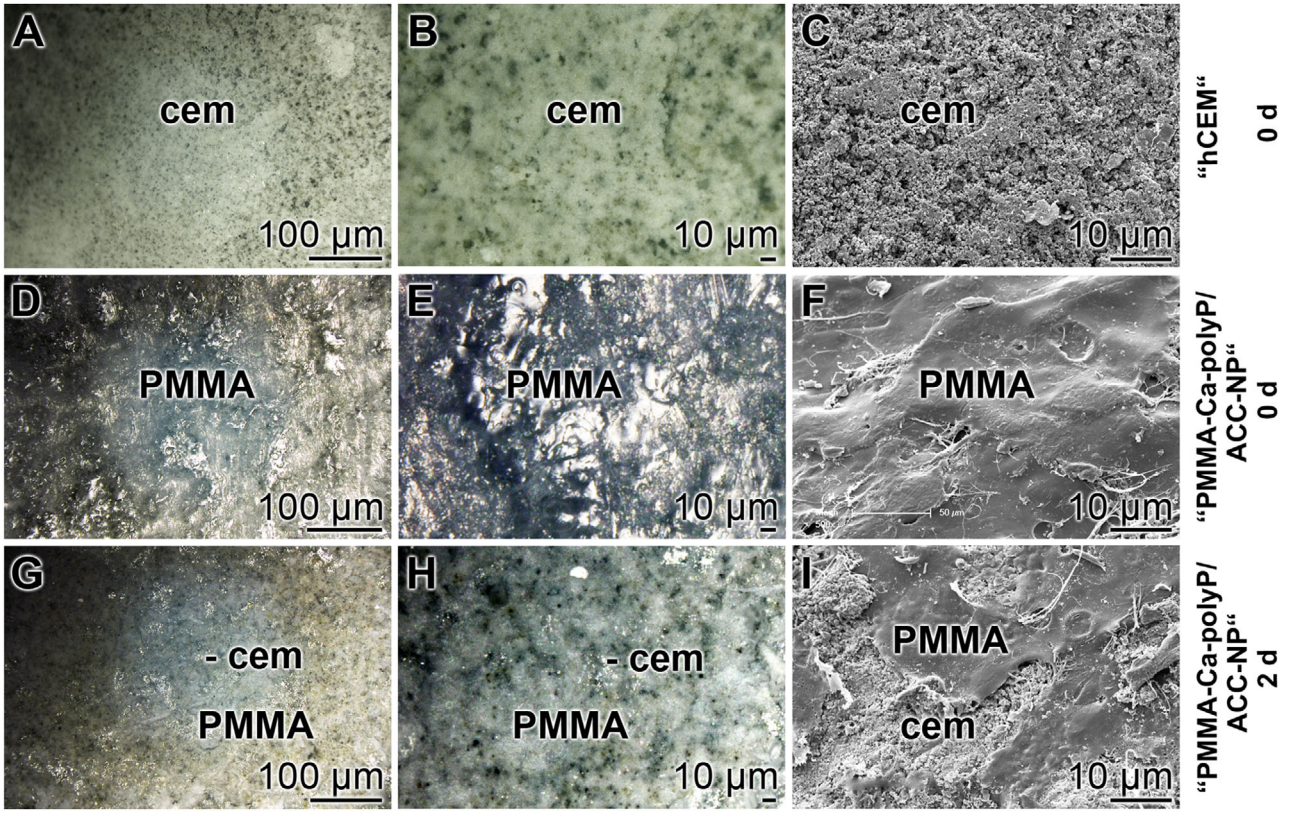


**Figure 5.** Susceptibility of the PMMA layer onto cement blocks toward water. The "hCEM" blocks were prepared and the cement remained either unprocessed (A–C) or was subsequently coated with "PMMA-Ca-polyP/ACC-NP" (D–I). C,F,I) ESEM and A,B,D,E,G,H) light microscopy. The samples were inspected either A–F) immediately (1 h) after coating or G–I) were submersed in water for 2 days. In the latter specimens, the continuous PMMA layer (PMMA) ruptures and allows the exposure of the cement (cem) cushion.

non-coated "hCEM" shows often a non-linear increment of the curve during the loading phase (Figure 8A, solid line). This property is attributed to the occurrence of (micro-) cracks, which are created during the loading phase. When the maximal load of ≈6 mN is reached, the curve has a creep of around 80 nm. During unloading, a small and incomplete recovery is detectable. The values measured for the cement control are 0.24 ± 0.12 GPa for HM and 10.26 ± 4.47 GPa for Er. The coating with the "PMMA" solution containing only the polymer causes a significant decrease of both the surface hardness as well as the reduced Young's modulus (Figure 8A, dashed line). The maximal load needed to attain the indentation depth is ≈4 mN, considerably lower if compared to the untreated cement control. However, the ascending curve during loading reflects a smooth continuous increment without discontinuities. At the maximal load, again, a creep phase is detectable. Here, the extent of creep is with 210 nm, more than twice as much higher than the one measured for "hCEM". Upon unloading, a distinct recovery phase is seen, which comprises almost the complete deformation observed during the holding period. These properties are also reflected by the measured values for HM (0.15 ± 0.026 GPa) and Er (5.32 ± 0.68 GPa) and indicate that a treatment with PMMA results in a reduction of the surface hardness which is paralleled with an increased surface elasticity.

The load/displacement curve for the cement coated with "PMMA-Ca-polyP/ACC-NP" shows a considerably different behavior (Figure 8A, dotted line) in comparison to "hCEM" and the "PMMA" coated cement. Here, a load of ≈8 mN is needed to reach the indentation depth of 1 µm. This is twice as much as that needed for the "PMMA" coated sample and one-third more than for the untreated cement control. The ascending curve is straight and without any discontinuities. After reaching the maximum load, a distinct creep phase is detected. The creep is comparable to the one measured for the "PMMA" coated sample and with ≈220 nm, again significantly higher than the one measured for the untreated cement control. The recovery phase upon unloading comprises almost the complete deformation range observed during the creep phase. The step within the curve, which is documented at the end of the recovery phase is most likely due to the building up of a strain incident causing a detaching of the diamond indenter. For the "PMMA-Ca-polyP/ACC-NP"-coated sample, the curve characteristics are 0.25 ± 0.1 GPa (HM) and 7.81 ± 2.22 GPa (Er). Taken together, addition of "Ca-polyP/ACC-NP" to the PMMA polymer ends up in a more rigid coating which mimics the surface hardness of unmodified cement. The measured HM values for the unmodified cement control "hCEM" as well as the "PMMA-Ca-polyP/ACC-NP"-coated sample are matching. Additionally, the coating with "PMMA-Ca-polyP/ACC-NP" results in a higher surface elasticity if compared to the cement control.

 

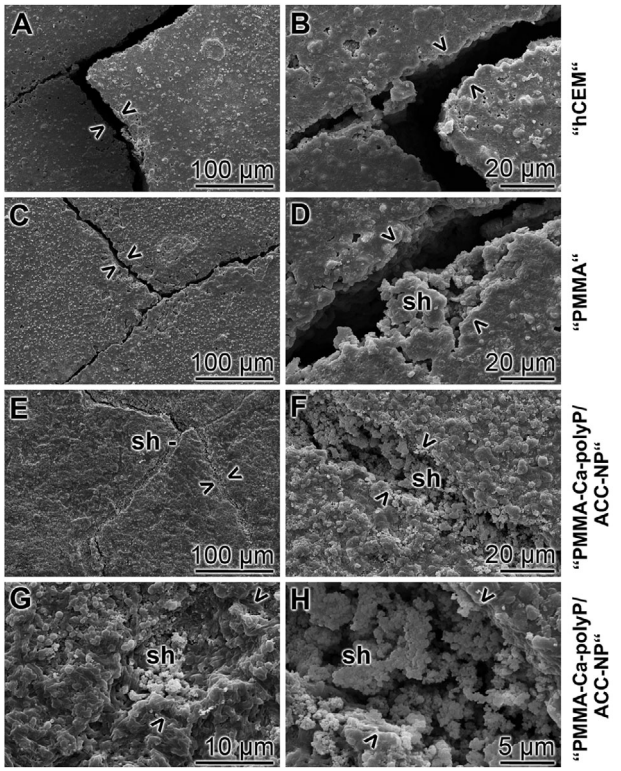


**Figure 6.** Closure of microcracks, introduced into "hCEM." The hardened cement paste samples remained either A,B) untreated as "hCEM", or were overlayed with C,D) "PMMA" or with E–H) "PMMA-Ca-polyP/ACC-NP" by brushing the polymer onto the surfaces. After evaporation of the solvent, the cement specimens were incubated in a humid chamber for 10 days. While in the untreated cement (A,B) no signs of self-healing are seen, self-healing (sh) deposits, in their initial phase, could be visualized in the "PMMA" (C,D) and, in an extensive manner, in the "PMMA-Ca-polyP/ACC-NP" (E–H) coated samples. The cracks are highlighted (> <).

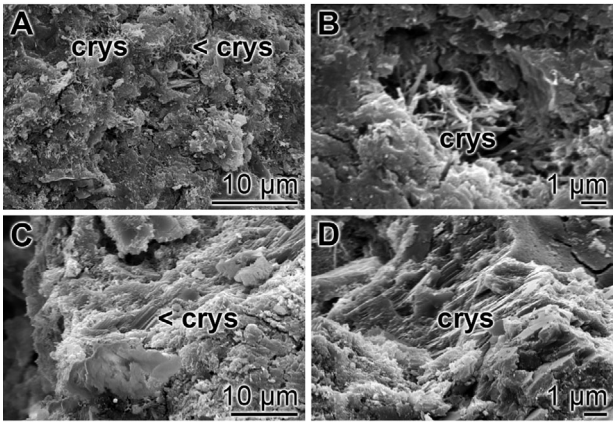


**Figure 7.** Crystal structures (crys) within the deposits formed during the self-healing within the microcracks treated with "PMMA-Ca-polyP/ACC-NP" polymer solution; ESEM. The crystal structures have a morphology similar to ettringite or also calcite.

### 2.3. Application of the Nanoparticles/PMMA by Blow Spinning

The blow spinning technology is suitable to overlay nano- as well as micro-composites with organic polymer-based materials, like polyvinylidene fluoride[38] or—like in the present study—PMMA.

#### *2.3.1. Surface Coating*

In a second approach, the cement blocks were coated by blow spinning with the mentioned polymer formulations in chloroform. The polymer formulations were loaded into the reservoir and then sprayed onto the cement material, as described under "Experimental Section." A scheme of the process is given in **Figure 9**C. The dissolved PMMA in the spray gun, which has—where mentioned—been supplemented with the nanoparticles, was sputtered out of the nozzle (Figure 9A) with high pressure onto the cement. In those experiments, the polymer solidified within 40 s, and if "PMMA-Ca-polyP/ACC-NP" is used, the nanoparticles are formed in close association with the PMMA fibers (Figure 9B). As sketched in Figure 9C (lower panel), hydrolysis of the polyP via the enzyme ALP from bacteria settling on the cement surface results in the dissolution of the particles and finally the formation of calcite crystals (Figure 9E; for comparison, the non-treated cement surface is shown in Figure 9D) (see under Section 3).

#### *2.3.2. Association of the PMMA-Based Blown Polymer Layer on the Cement Surface*

If the PMMA polymer, administered as "PMMA" or as "PMMA-Ca-polyP/ACC-NP," is blown as unstable droplets onto the cement surface (**Figure 10**A,B), fibers of the polymer developed after the evaporation of the solvent are seen onto the cement (Figure 10C,D). Those fibers are associated with the polyP nanoparticles if "PMMA-Ca-polyP/ACC-NP" is used (Figure 10E,F). If those cement blocks are submersed into water for 2 days, those fibers disintegrate and liberate a tightly attached polymer coat onto the surface of the cement (Figure 10G,H).

### 2.4. Supplementation of Biodentine (bone grafting material) with polyP

The silicate–carbonate cement for biomedical application, "BD," was processed without polyP or with either 0.5% wt/wt Na-polyP or 0.5% wt/wt "Ca-polyP-NP" and then subjected for analysis.

#### *2.4.1. Morphology of the Surface*

The surface of the untreated "BD" showed a coarse appearance (**Figure 11**A–C). Addition of Na-polyP, prior to the hardening with Ca-chloride solution, results in a much smoother surface of the "BD-Na-polyP" cement and hardly leaves open coarse crystal-like particles (Figure 11D–F). Even smoother is the surface of the "BD-Ca-polyP-NP" (Figure 11G–I). A closer inspection of the surface texture shows a dense and velvet-like character filled with densely arranged nanoparticles.

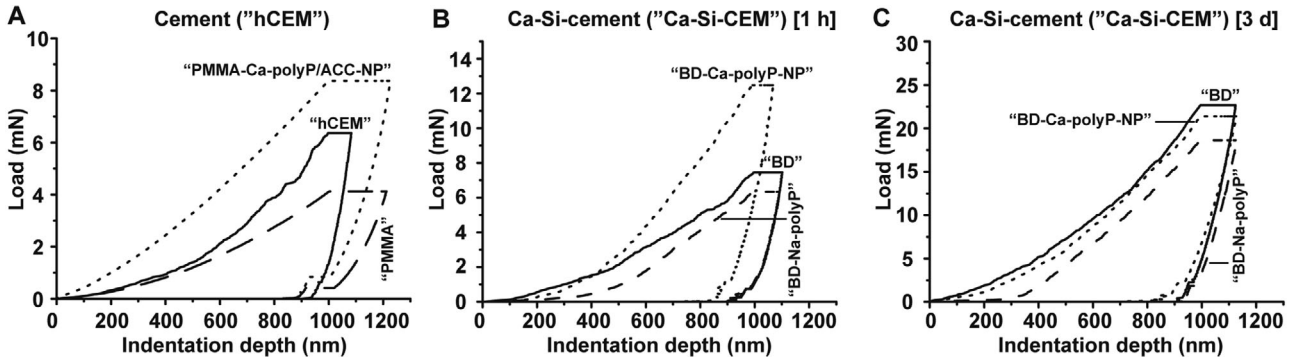


**Figure 8.** Characteristic load-displacement curves from indentation experiments with A) cement and B,C) the calcium silicate cement [Ca-Si-CEM] (Biodentine), directly 1 h after mixing, or after an aging of 3 days, respectively. A) The cement samples remained either uncoated ("hCEM") (solid line) or were coated with "PMMA" (broken line) or with "PMMA-Ca-polyP/ACC-NP" (dotted line). B,C) The biodentine samples were either untreated ("BD") (solid line) or were supplemented with Na-polyP ("BD-Na-polyP") (broken line) or with Ca-polyP-NP ("BD-Ca-polyP-NP") (dotted line).

*2.4.2. Mechanical Properties*

The nanoindentation measurements were performed as outlined under "Experimental Section." In Figures 8B (measurement after 1 h) and 8C (3 days), representative load/displacement curves for the three different specimens "BD," "BD-Na-polyP," and "BD-Ca-polyP-NP" are shown. Since the material hardens with time, two time points have been selected for the determinations: 1 h after completion of the mixing of the components and 3 days later.

One hour after preparation (Figure 8B), the controls, "BD," show a slightly fluttering curve progression during the loading phase. We attribute this progression to the occurrence of (micro-) cracks upon loading. When the maximal load of ≈7.5 mN is reached, the curve shows a creep behavior of ≈100 nm. During unloading, a small and incomplete recovery phase of ≈200 nm is detectable. The measured values for the "BD" control are 0.29 ± 0.15 GPa for HM and 15.19 ± 5.03 GPa for Er, respectively (Figure 8B, solid line). Addition of Na-polyP to the cement, "BD-Na-polyP", results in a slight decrease of both the surface hardness as well as the reduced Young's modulus (Figure 8B, dashed line). The maximal load needed to attain the indentation depth is with ≈6.4 mN, significantly lower if compared to the control. At a maximal load, a creep phase showing an almost identical progression as in the control is measured. Upon unloading, a distinct recovery phase of again nearly 200 nm is visible. The described observations are also reflected by the measured values for HM (0.26 ± 0.16 GPa) and Er (13.79 ± 7.22 GPa). These data imply that an inclusion of Na-polyP into the cement leads to a decreased surface hardness together with an increased surface elasticity. The modified biodentine is thus slightly softer but simultaneously more elastic than the original material. The general courses of the load/displacement curves are almost identical to each other. In contrast to "BD-Na-polyP", biodentine supplemented with Ca-polyP NP, for "BD-Ca-polyP-NP", the respective curve reflects a considerably higher needed load of almost 12.5 mN to reach the indentation depth of 1 µm. After reaching the maximum load, a distinct creep phase occurs which is with ≈70 nm significantly lower than those determined for the other two samples. Furthermore, the recovery phase upon unloading is again with >300 nm, much more pronounced. For the "BD-Ca-polyP-NP" specimen, the key parameters are 0.49 ± 0.21 GPa (HM) and 19.27 ± 6.87 GPa (Er). In turn, addition of "Ca-polyP-NP" to biodentine causes an increase of the mechanical properties of biodentine, since this material shows a higher surface hardness and also a higher stiffness compared to the unmodified biodentine cement.

The measurements after 3 days (Figure 8C): Under those conditions, a significant increase of the parameters HM and Er is measured. With respect to the biodentine control, the hardness increases to >300% (HM: 0.9 ± 0.24 GPa and for the Er to 32.48 ± 8.5 GPa); simultaneously, a higher indentation depth with a load of 22.5 mN is also determined. For the "BD-Na-polyP" cement, the HM increases to 0.73 ± 0.16 GPa, while concurrently the Er increases to 25.02 ± 7.94 GPa. A load of ≈18.75 mN is needed to reach the chosen indentation depth. In comparison to the characteristics measured immediately (1 h) after mixing of the components, after a 3-day hardening period, the "BD-Na-polyP" cement is slightly softer and more elastic compared to the untreated control. Finally, the "BD-Ca-polyP-NP" sample has a higher HM (0.92 ± 0.16 GPa; +188%) and likewise also a higher Er with 32.29 ± 7.06 GPa. For this sample, a load of ≈21.25 mN is needed to achieve the present indentation depth. These data show that the "BD-Ca-polyP-NP" specimen does not change the mechanical properties as much as seen in comparison to "BD-Na-polyP." Taken together, the control material after an aging time of 3 days is considerably harder and stiffer compared to the polyP supplemented cement samples ("BD-Na-polyP"; "BD-Ca-polyP-NP") at the beginning of the hardening period.

## 3. Discussion

The role of cement for construction and also reconstitution of buildings is different from the function of cement in oral dental care and hygiene. This latter objective is also applicable for reconstitution and regeneration of bone in general. In the first case, application as construction material, it is paramount that the cement acts and meets not only the mechanical constraints but—in the long run—also the inherent need of self-healing. In the latter scenario, the cement needs to act as a biogenic, biocompatible, and regeneratively active material, allowing a

 

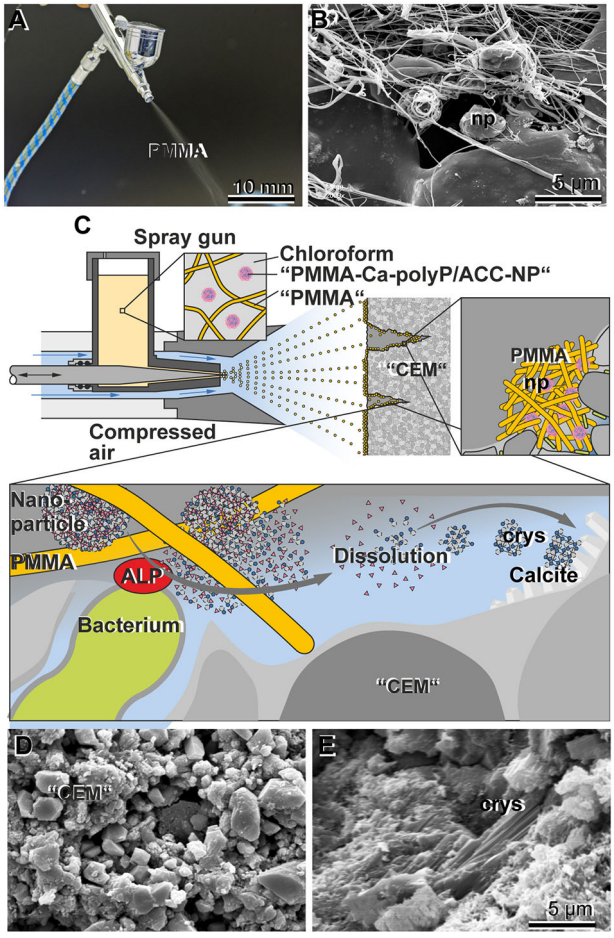


**Figure 9.** Schematic set-up of the blow spinning airbrush device. A) The airbrush with the spray gun and the shooted out PMMA-based polymer that has been used for surface coating. B) Polymer fibers with the associated nanoparticles (np). C) Upper panel: Airbrush consisting of the spray gun connected to the dispenser and the 0.5 mm nozzle spraying "PMMA-Ca-polyP/ACC-NP" or "PMMA" onto the cement "hCEM" with the surface-associated cracks. The cracks become filled with PMMA and nanoparticles (np). lower panel: On the cement surface the bacteria, via ALP, enzymatically hydrolyze polyP followed by the dissolution of the particles. Subsequently, the released ACC undergoes crystallization (cryst) to calcite. D) Cement ("hCEM") surface. E) Cement surface coated with "PMMA-Ca-polyP/ACC-NP" which gives rise to calcite-based crystals (crys).

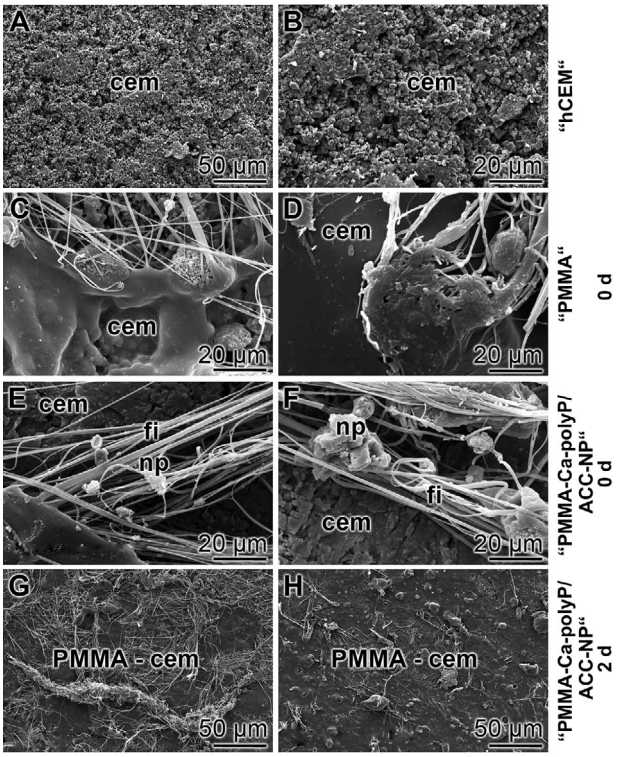


**Figure 10.** Blowing of the PMMA-polymer onto the cement, using the airbrush device; ESEM. A,B) Untreated cement surface. Surface of a cement block onto which either C,D) "PMMA" or E,F) "PMMA-Ca-polyP/ACC-NP", containing the nanoparticles (np) has been administered with the spray gun; view at day 0. G,H) Surface of a "PMMA-Ca-polyP/ACC-NP"-coated cement (cem) sample after submersion into water for 2 days. The polymer is seen as a tightly attached film onto the cement (PMMA–cem).

self-repair of bone. In the present study, polyP was either added as a water-soluble Na-polyP salt or as water insoluble, but serum dissolvable,[39] Ca-polyP nanoparticles. During both remediation processes (construction/reconstitution of buildings and dental/bone repair), two biological players are required: bacteria and, only in the latter case, biological body fluids. A similar approach has been proposed earlier by showing that microbial calcite precipitation contributes to remediation of surfaces and subsurfaces of porous media.[40] The inclusion of bacteria into cement construction material, termed biocementation, has been extensively stressed by the group of Cabalar.[41]

Focusing on the role of cement as construction or conservation/repair material for buildings, it is shown that especially the cement components used for present-day buildings suffer from the lack of a self-healing property. This holds true particularly for monuments/buildings that have been built after World War II.[42] As outlined in Section 1, one difference between more recent buildings and antique constructions (Figure 1) is that the more recent cements have a lower content of Ca-carbonate/phosphate. In the present study, we applied PMMA, a proven coating material,[43] as a vehicle and introduced it together with a combination of amorphous Ca-polyP nanoparticles, "Ca-polyP-NP", and polyP-stabilized amorphous Ca-carbonate, "ACC-NP", as essential components for the coating of cement, providing this binder with self-healing properties. A scheme, summarizing the function of the polyP-stabilized ACC nanoparticles, "ACC-NP", present in "PMMA-Ca-polyP/ACC-NP" formulation is sketched in **Figure 12**. The particles combine the three cornerstones for a successful self-healing of cracked materials: polyP, Ca-carbonate, and the presence of this components as amorphous NP. The authors are aware that in this study comparably small microcracks have been targeted. Such small cracks are, however, imperative initiators for larger defects, especially in historic monuments that lack any iron/steel reinforcement.[44] The introduced innovative material "PMMA-Ca-polyP/ACC-NP" relies on the inherent self-healing activity of its components, amorphous Ca-carbonate (ACC) and polyP; the processing of these components is dependent on the presence of the bacteria which are ubiquitously found in large quantities both in the air and in the aqueous milieu,[45] as well as on cement surfaces.[46]

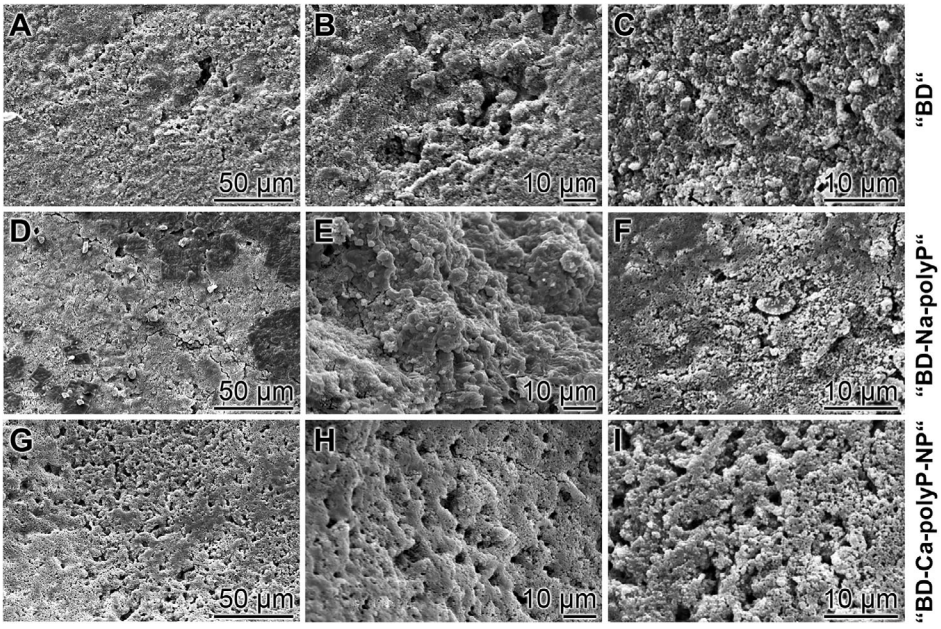


**Figure 11.** Surface morphology of biodentine cement. The material remained A–C) non-supplemented, "BD", or was mixed with D–F) Na-polyP, "BD-Na-polyP", or with G–I) Ca-polyP-NP, "BD-Ca-polyP-NP"; ESEM.

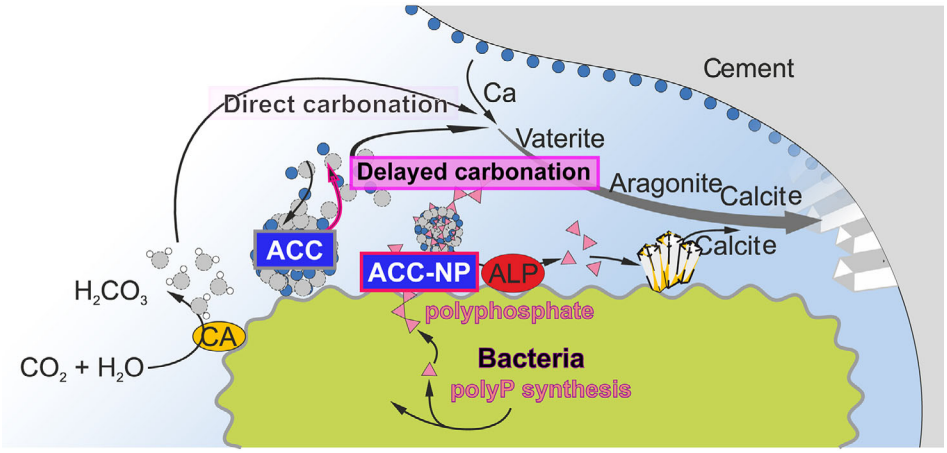


**Figure 12.** Scheme showing the role of the polyP-stabilized ACC nanoparticles, "ACC-NP" in delayed carbonation of cement. In the absence of polyP, the amorphous phase of Ca-carbonate, ACC, is readily converted to the more stable crystalline phases, vaterite and aragonite, and finally calcite ("direct carbonation"). The function of polyP in stabilizing the amorphous particles "ACC-NP" is abolished after enzymatic hydrolysis of polyP by the ALP enzyme present on the surface of bacteria, resulting in a delayed formation of calcite crystals on the cement surface ("delayed carbonation"). Ca-carbonate can also be formed via the bacterial carbonic anhydrase.

### 3.1. Amorphous Ca-Carbonate

ACC is the precursor and the starting component during crystallinic calcite, aragonite, and vaterite formation, which initiates, supports, and accelerates carbonation of cement, also in biological systems.[25,26] In the particles used for the experiments reported here, ACC has been encapsulated in a polyP scaffold which stabilizes ACC, the amorphous phase of Ca-carbonate.[13] This role of polyP is abolished after enzymatic hydrolysis of polyP via the ALP, an enzyme that is present on the surface of bacteria.[47,48] In the absence of polyP, ACC is readily transformed along the thermodynamic route to calcite, the final stabilizing crystals in the cement:[49] "direct carbonation." As outlined in Figure 12, the process of ACC-NP-driven calcite formation/carbonation is termed "delayed carbonation. In addition, the introduction of ACC to the cement system allows a substitution of the Ca-carbonate which is fabricated by the bacterial carbonic anhydrase.[50]

### 3.2. Polyphosphate

It might be stressed that polyP is also a product from bacteria and serves as a single molecule as an accelerator of cement

 

self-healing.[19] In addition, as reported previously, the orthophosphate produced during enzymatic degradation of the polymeric polyP, both from the amorphous Ca-polyP NP and, as introduced here, the ACC-NP, by the ALP from bacteria residing on the cement/crack surfaces, can precipitate as Ca-phosphate,[19] a process that will additionally contribute to the self-healing of cracks occurring in concrete.

It is indicative that the polyP-based nanoparticles, "Ca-polyP/ACC-NP," if applied on the surface of construction cement increase the rigidity of the treated area to a value that matches the characteristics of the adjacent (untreated) cement. Thereby, the polyP-enriched PMMA, "PMMA-Ca-polyP/ACC-NP", compensates for the transitional reduction of the hardness measured for PMMA alone.

These data imply that the "PMMA-Ca-polyP/ACC-NP" coating solution containing "Ca-polyP/ACC-NP" particles can serve as a novel bioinspired or bioimitating material with self-healing potential for the reconstruction/repair of buildings, in particular micro-cracks occurring in historic monuments. If applied to the cement, both by brushing or by blow spinning, the PMMA polymer mixed with "Ca-polyP/ACC-NP" shows a considerable power to become integrated into the cement. The data suggest that the polyP-based supplement contributes to an increased calcite formation, which is conceivable.

As an example for cement applicable in oral dental care and hygiene, the biodentine was used in the present study. This material readily allows the integration of the polyP polymer, especially of the soluble Na-polyP salt (as "BD-Na-polyP") and—to a lesser extent—of "Ca-polyP-NP" (as "BD-Ca-polyP-NP"). Both polyP formulations smoothen the surfaces of the calcium-silicate-based biodentine material. In the series with Ca-polyP NP, the surface coat of the biomedical cement even exposes nanoparticles. The determination of the biomechanical properties of biodentine revealed that addition of polyP, as soluble Na-polyP, results in a slightly softer and simultaneously more elastic material compared to the untreated control and especially to the Ca-polyP-NP supplemented $Ca^{2+}$/silicate biodentine which has an almost twofold higher hardness than the control. This property is seen almost immediately after mixing of the starting components, after 1 h. After 3 days, the surface hardness and the stiffness of the control without polyP significantly increase. At this point, however, the initial increase in these properties of the Ca-polyP-NP supplemented biodentine with respect to the control is no longer observed, and more importantly, the decrease in surface hardness and the increase in surface elasticity of the Na-polyP supplemented biodentine is even more pronounced compared to the control than shortly after the mixing of the components. This property reflects a hybrid-like formation between the coarse calcium-silicate-based cement particles and the nanosized polymer polyP. Recently, a migration of $Ca^{2+}$ between polyP and Ca-rich crystals, similar to biodentine (rich in tricalcium silicate and Ca-carbonate[29]), has been described for the two components Na-polyP and hydroxyapatite.[31] The new material properties of the polyP supplemented $Ca^{2+}$/silicate biodentine material to be slightly less hard and simultaneously more elastic appear to be favorable for bone and teeth implants in order to avoid brittleness.[51]

## 4. Conclusion

Cements, both for construction of monuments/buildings and for biomedical applications, especially in the oral dental field, are based on the same phases, tricalcium silicate, dicalcium silicate, ferrite, and sulfate. Portland cement contains in addition tricalcium aluminate. In parallel, biodentine used for medical application and a similarly composed construction cement were studied. It was found that the hardening and the flexibility of these materials are initiated and subsequently maintained by a rapid growth of C-S-H (calcium-silicate-hydrate) as well as by the formation of calcite. The new data summarized here broaden and supplement our previous findings that addition of amorphous Ca-carbonate together with polyP nanoparticles accelerates the self-healing potential both of construction cement and of cement for bio-medical applications. The application and addition of the polyP-based particles to the differently directed cement formulations improve the self-healing potency of construction cement and also the stability of cement used as implant material for bone and dental applications.

## 5. Experimental Section

*Materials*: Na-polyphosphate (Na-polyP) with an average chain length of 40 phosphate units was purchased from Chemische Fabrik Budenheim (Budenheim; Germany). Portland cement, CEM I 42.5 R, was a gift of HeidelbergCement AG (Mainz, Germany—Dr. Ulrich Schneider). Analysis of the batch used (LN 43308/001) revealed the following composition: $Ca_3SiO_5$, $\alpha$-$Ca_2SiO_4$, $\beta$-$Ca_2SiO_4$, aluminate [$Ca_3Al_2O_6$], calcium aluminoferrite [$Ca_2(Al,Fe)_2O_5$], $K_2SO_4$, MgO, CaO, $Ca(OH)_2$, $CaSO_4$, $CaSO_4 \bullet 0.5 H_2O$, $CaCO_3$, $SiO_2$, and $CaMg(CO_3)_2$. The percentage distribution of the components has been given earlier.[19] Biodentine was purchased from Septodont GmbH (Niederkassel, Germany).

*Preparation of the Nanoparticles: Amorphous Ca-polyP Nanoparticles*: The Ca-polyP (Ca-polyphosphate) nanoparticles were prepared as described before.[19].

*Preparation of the Nanoparticles: Amorphous Calcium Carbonate Nanoparticles*: The particles were prepared as outlined before.[13] The particles were collected, washed with acetone, and dried at room temperature; "Ca-polyP/ACC-NP."

*Preparation of Cement Samples*: The unhydrated cement was termed "CEM." A sample of 100 g was supplemented with 38 g of distilled water and mixed thoroughly. During the blending period, the temperature increased slightly to ≈28 °C.

The cement samples were prepared either in 30 mm circular plastic molds (thickness of the layers: 10 mm) or in 15 mm molds (height: 8 mm) and allowed to harden for 10 days prior to analysis; during this period, the specimens remained in a humidity chamber (humidity: ≈20 g $m^{-3}$) at room temperature (20 °C). Then, the samples were transferred to room humidity (at 20 °C) for 1 day and used for the experiments. The hardened cement paste was termed "hCEM."

*Formulation of the PMMA-Based and polyP-Supplemented Cement Coating Solution*: The acrylic glass PMMA (5 w/v%) (#182265; Sigma-Aldrich) was dissolved in chloroform (#A3633; AppliChem, Darmstadt; Germany) at 50 °C under stirring for 2 h. This solution was termed "PMMA."

In parallel, the "PMMA" solution was supplemented with 10 w/w% "Ca-polyP/ACC-NP" (based on PMMA) and ultrasonicated in a water bath (Grant Instruments, Cambridge; UK) at room temperature; "PMMA-Ca-polyP/ACC-NP."

*Application of "PMMA" or of "PMMA-Ca-polyP/ACC-NP": Brush Coating*: The processed and hardened cement samples were coated with either "PMMA" or "PMMA-Ca-polyP/ACC-NP" using a 30 mm wide paint

roller–texture roller (Huawei Paint Brush, Beijiao; China). Approximately 0.3 mL of the material was applied onto the 700 $mm^2$ cement area.

In order to study the durability of the homogeneous PMMA layer, the "PMMA" treated cement specimens were submersed in tap water for 2 days and then inspected microscopically.

*Application of "PMMA" or of "PMMA-Ca-polyP/ACC-NP": Blow Spinning*: The "PMMA" or the "PMMA-Ca-polyP/ACC-NP" solution was loaded to a Timbertech Airbrush (Airgoo Pneumatic, Emmen, The Netherlands) with a diameter of the nozzle of 0.5 mm. The dispenser was connected with an ABPST05 compressor, combined with an air pressure regulator gauge and a water trap filter. The respective solutions were sprayed at a distance of 10 cm onto a round-shaped substrate (cement or glass microscope slide) as outlined.[38,52] An area of 6.75 $cm^2$ was sprayed for 2 min with 2 mL of the respective solution to completely cover the surface. The samples were kept at room temperature overnight to allow evaporation of residual solvent.

*Microcrack Formation and Self-Healing Analysis*: Microcracks were introduced into "hCEM" (after an aging of 10 days) by freezing–thawing cycles of −80 °C (for 60 min) to +60 °C (60 min), separated by short submersion steps. Five cycles were applied.[19] The sizes of the microcracks, introduced by freezing–thawing cycles, varied within the range ≈15 and ≈58 µm (average: 44 ± 13 µm; 25 independent determinations). The dimensions have been determined by using the "Celleste Image Analysis Software" (Thermo Fisher Scientific, Dreieich, Germany).

Subsequently, the samples remained submersed in water whose level reached 3 mm below the top edge of the blocks. The samples remained like this for 10 days prior to microscopic inspection and further analyses.

*Determination of the Mechanical Properties*: The mechanical properties of the coated as well as the non-coated cement samples were determined by using the nanoindenter system from NanoTest Vantage (Micro Materials Ltd, Wrexham, UK) equipped with a Berkovich diamond indenter.[53] This device allows a continuous depth-sensing nanoindentation. For each sample, at least 50 independent indentation determinations were performed. The following conditions were applied: temperature 25 °C, maximum depth limit 1 µm, loading/unloading rate 0.3 mN $s^{-1}$, as well as a holding period at maximum load for 30 s. The distance between two adjacent indents was at least 30 µm. Based on the measured raw data, the Martens hardness (HM) as well as the reduced Young's modulus (Er) were calculated according to the described procedure.[53] All calculations were performed with the Nano-Test Platform Four V.40.08 software package (Micro Materials Ltd). The data was recorded at a continuous recording frequency of 50 Hz using the Emperor XT Force software (Mecmesin, Slinfold, Horsham; UK). A force of 0.5 N was found to be suitable to determine the compressive strength during the measurements.

*Biodentine and the polyP Supplementation*: Biodentine (BD) is made of two different components, first a powder, composed of tricalcium silicate and dicalcium silicate as core material, and second calcium carbonate and oxide as filler.[30] The cement material was hardened with a Ca-chloride solution as a "setting agent," as described in the Instructions. Usually, the setting time was 12 min; "BD." The determinations were performed with the Gillmore Needle Apparatus (Gilson Germany, Limburg-Offheim).

In parallel series, Na-polyP or "Ca-polyP-NP" in a concentration of 0.5% wt/wt based on the dry weight was added to the powder. After crushing for 5 min (pestle/mortar), a homogeneous solid mixture was obtained that was hardened with the Ca-chloride solution in a Teflon mold (diameter of 3 mm; thickness of 10 mm). The obtained biodentine disks were then air-dried for 1 day or longer as mentioned in the experiments, and then used for the studies; "BD-Na-polyP" or "BD-Ca-polyP-NP."

*Microscopic Analyses*: The electron microscopic images were obtained either with a scanning electron microscope, a HITACHI SU8000 electron microscope (Hitachi, Krefeld, Germany), or with an ESEM, using an ESEM XL-30 apparatus (Philips, Eindhoven, Netherlands), as described.[54] Light microscopical images were taken with a VHX-600 Digital Microscope from Keyence (Neu-Isenburg; Germany).

*Statistical Analysis*: After finding that the values follow a standard normal Gaussian distribution, the results were statistically evaluated using the paired Student's *t*-test.[55]

## Acknowledgements

The authors thank Ms. Kerstin Bahr (Electron Microscopy), Institute of Functional and Clinical Anatomy, University Medical Center Mainz (Germany), for continuous support. W.E.G.M. is the holder of an ERC Advanced Investigator Grant (grant No. 268476). In addition, W.E.G.M. obtained three ERC-PoC grants (Si-Bone-PoC, grant No. 324564; MorphoVES-PoC, grant No. 662486; and ArthroDUR, grant No. 767234). Finally, this work was supported by grants from the European Commission (Bio-Scaffolds and InnovaConcrete; grant Nos. 604036 and 760858) and the BiomaTiCS research initiative of the University Medical Center, Mainz.

Open access funding enabled and organized by Projekt DEAL.

## Conflict of Interest

The authors declare no conflict of interest.

## Keywords

amorphous calcium carbonate, cement, inorganic polyphosphate, nano/microparticles, self-healing

Received: March 28, 2020
Revised: May 12, 2020
Published online: July 1, 2020

[1] Ö. Kirca, *Proc. of the IVth Int. Seminar on Structural Analysis of Historical Constructions* (Eds: C. Modena, P. B. Lourenço, P. Roca), CRC Press, London **2005**, p. 87.
[2] A. M. Raymond, *Notes Pratiques Et Résumés Sur L'art Du Constructeur En Turquie*, Typolithographie central, Della Rocca, Alexandrie **1908**, p. 100.
[3] *TMM_CH 2018* (Eds: A. Moropoulou, M. Korres, A. Georgopoulos, C. Spyrakos, C. Mouzakis), Springer Press, Berlin **2019**, p. 421.
[4] C. Oguz, F. Turker, N. U. Kockal, *Sci. World J.* **2014**, *2014*, 536105.
[5] M. Cao, X. Ming, K. He, L. Li, S. Shen, *Materials* **2019**, *12*, 781.
[6] X. Xu, L. Wang, *Adv. Cem. Res.* **2018**, *30*, 185.
[7] S. Wei, Z. Jiang, H. Liu, D. Zhou, M. Sanchez-Silva, *Braz. J. Microbiol.* **2014**, *44*, 1001.
[8] T. T. H. Bach, C. Cau-Dit-Coumes, I. Pochard, A. Nonat, *Cem. Concr. Res.* **2013**, *51*, 14.
[9] A. Lotsari, A. K. Rajasekharan, M. Halvarsson, M. Andersson, *Nat. Commun.* **2018**, *9*, 4170.
[10] X. H. Wang, H. C. Schröder, W. E. G. Müller, *J. Mater. Chem. B* **2018**, *6*, 2385.
[11] X. H. Wang, H. C. Schröder, K. Wang, J. A. Kaandorp, W. E. G. Müller, *Soft Matter* **2012**, *8*, 9501.
[12] W. E. G. Müller, H. C. Schröder, X. H. Wang, *Chem. Rev.* **2019**, *119*, 12337.
[13] E. Tolba, S. F. Wang, M. Neufurth, M. Ackermann, R. Muñoz-Espí, B. M. Abd El-Hady, H. C. Schröder, W. E. G. Müller, *Molecules* **2020**, *25*, 2360.
[14] W. E. G. Müller, E. Tolba, H. C. Schröder, X. H. Wang, *Macromol. Biosci.* **2015**, *15*, 1182.
[15] I. S. Kulaev, V. Vagabov, T. Kulakovskaya, *The Biochemistry of Inorganic Polyphosphates*, John Wiley, Chichester, England **2004**.
[16] J. H. Morrissey, S. H. Choi, S. A. Smith, *Blood* **2012**, *119*, 5972.
[17] W. E. G. Müller, E. Tolba, H. C. Schröder, S. Wang, G. Glaßer, R. Muñoz-Espí, T. Link, X. H. Wang, *Mater. Lett.* **2015**, *148*, 163.
[18] R. Docampo, W. de Souza, K. Miranda, P. Rohloff, S. N. Moreno, *Nat. Rev. Microbiol.* **2005**, *3*, 251.

 

[19] W. E. G. Müller, E. Tolba, S. Wang, Q. Li, M. Neufurth, M. Ackermann, R. Muñoz-Espí, H. C. Schröder, X. H. Wang, *Int. J. Mol. Sci.* **2019**, *20*, 2948.
[20] T. Matschei, B. Lothenbach, F. P. Glasser, C C Res. **2007**, *37*, 551.
[21] I. Labidi, S. Boughanmi, A. Khelidj, M. El Maaoui, A. Megriche, *Chem. Africa* **2019**, *2*, 401.
[22] J. Davidovits, *Concrete Intern.* **1987**, *9*, 23.
[23] D. M. Roy, C. A. Langton, *Mat. Res. Soc. Symp. Proc.* **1984**, *26*, 543.
[24] X. H. Wang, M. Ackermann, S. Wang, E. Tolba, M. Neufurth, Q. Feng, H. C. Schröder, W. E. G. Müller, *Biomed. Mater.* **2016**, *11*, 035005.
[25] X. H. Wang, H. C. Schröder, W. E. G. Müller, *Trends Biotechnol.* **2014**, *32*, 441.
[26] W. Liu, Y. Q. Li, L. P. Tang, Z. J. Dong, *Mater. Today Commun.* **2019**, *19*, 464.
[27] M. Mamlouk, J. Zaniewski, *Materials for Civil and Construction Engineers*, Addison Wesley Longman, Harlow, England **1999**.
[28] X. V. Tran, C. Gorin, C. Willig, B. Baroukh, B. Pellat, F. Decup, S. Opsahl Vital, C. Chaussain, T. Boukpessi, *J. Dent. Res.* **2012**, *91*, 1166.
[29] M. Kaur, H. Singh, J. S. Dhillon, M. Batra, M. Saini, *J. Clin. Diagn. Res.* **2017**, *11*, ZG01.
[30] Ö. Malkondu, M. K. Kazandağ, E. Kazazoğlu, *Biomed Res. Int.* **2014**, *2014*, 160951.
[31] W. E. G. Müller, S. F. Wang, M. Ackermann, T. Gerich, M. Neufurth, M. Wiens, H. C. Schröder, X. H. Wang, *Adv. Funct. Mater.* **2019**, *29*, 1905220.
[32] J. J. Verhoef, A. D. Barendrecht, K. F. Nickel, K. Dijkxhoorn, E. Kenne, L. Labberton, O. J. McCarty, R. Schiffelers, H. F. Heijnen, A. P. Hendrickx, H. Schellekens, M. H. Fens, S. de Maat, T. Renné, C. Maas, *Blood* **2017**, *129*, 1707.
[33] A. J. Donovan, J. Kalkowski, S. A. Smith, J. H. Morrissey, Y. Liu, *Biomacromolecules* **2014**, *15*, 3976.
[34] H. N. Walker, D. S. Lane, P. E. Stutzman, Petrographic Methods of Examining Hardened Concrete: A Petrographic Manual, FHWA-HRT-04-150, U.S. Department of Transportation, Washington, DC **2006**.
[35] V. Rives, J. Garcia-Talegon, *Mater. Sci. Forum* **2006**, *514-516*, 1689.
[36] M. Deng, M. Tang, *Cement Concrete Res.* **1994**, *24*, 119.
[37] J. S. Belkowitz, D. Armentrout, *ACI Special Publication* **2009**, SP 267:87.
[38] J. Gonzalez-Benito, J. Teno, G. Gonzalez-Gaitano, S. Xu, M. Y. Chiang, *Polym. Test.* **2017**, *58*, 21.
[39] W. E. G. Müller, S. Wang, E. Tolba, M. Neufurth, M. Ackermann, R. Muñoz-Espí, I. Lieberwirth, G. Glasser, H. C. Schröder, X. H. Wang, *Small* **2018**, *14*, 1801170.
[40] S. Stocks-Fischer, J. K. Galinat, S. S. Bang, *Soil Biol. Biochem.* **1999**, *31*, 1563.
[41] A. F. Cabalar, Z. Karabash, O. Erkmen, *European Journal of Environmental and Civil Engineering* **2016**, *22*, 1238.
[42] H. A. Heinemann, *Case Stud. Constr. Mater.* **2017**, *7*, 207.
[43] T. Coan, G. S. Barroso, G. Motz, A. Bolzána, R. A. F. Machado, *Mater. Res.* **2013**, *16*, 1366.
[44] B. Šavija, M. Lukovic, J. Pacheco, E. Schlangen, *Constr. Build. Mater.* **2013**, *44*, 626.
[45] A. Barberán, K. S. Ramirez, J. W. Leff, M. A. Bradford, D. H. Wall, N. Fierer, *Ecology Lett.* **2014**, *17*, 794.
[46] A. Bertron, *Mater. Struct.* **2014**, *47*, 1787.
[47] B. Lorenz, H. C. Schröder, *Biochim. Biophys. Acta - Protein Struct. Mol. Enzymol.* **2001**, *1547*, 254.
[48] H. Luo, R. Benner, R. A. Long, J. Hu, *Proc. Natl. Acad. Sci. USA* **2009**, *106*, 21219.
[49] J. Jiang, Q. Zheng, D. Hou, Y. Yan, H. Chen, W. She, S. Wu, D. Guo, W. Sun, *Phys. Chem. Chem. Phys.* **2018**, *20*, 14174.
[50] A. F. Alshalif, J. M. Irwan, N. Othman, A. Al-Gheethi, A. Hassan, I. M. Nasser, *MATEC Web of Conf.* **2018**, *250*, 03004.
[51] R. B. Osman, M. V. Swain, *Materials* **2015**, *8*, 932.
[52] A. M. C. Santos, E. L. G. Medeiros, J. Blaker, E. S. Medeiros, *Mater. Lett.* **2016**, *176*, 122.
[53] W. C. Oliver, G. M. Pharr, *J. Mater. Res.* **1992**, *7*, 1564.
[54] A. Giacomini, M. Ackermann, M. Belleri, D. Coltrini, B. Nico, D. Ribatti, M. A. Konerding, M. Presta, M. Righi, *Angiogenesis* **2015**, *18*, 499.
[55] L. Sachs, *Angewandte Statistik*, Springer, Berlin **1984**, p. 242.

 